A Distribution Kinetics Approach for Crystallization of Polymer Blends

Jiao Yang

Department of Chemical Engineering, Louisiana State University, Baton Rouge, Louisiana 70803

Benjamin J. McCoy

Department of Chemical Engineering and Materials Science, University of California, Davis, California 95616

Giridhar Madras*

Department of Chemical Engineering, Indian Institute of Science, Bangalore 560 012, India

Received: April 21, 2006; In Final Form: June 7, 2006

The cluster distribution approach is extended to investigate the crystallization kinetics of miscible polymer blends. Mixture effects of polymer−polymer interactions are incorporated into the diffusion coefficient. The melting temperature, activation energy of diffusion, and phase transition enthalpy also depend on the blending fraction and lead to characteristic kinetic behavior of crystallization. The influence of different blending fractions is presented through the time dependence of polymer concentration, number and size of crystals, and crystallinity (in Avrami plots). Computational results indicate how overall crystallization kinetics can be expressed approximately by the Avrami equation. The nucleation rate decreases as the blending fraction of the second polymer component increases. The investigation suggests that blending influences crystal growth rate mainly through the deposition-rate driving force and growth-rate coefficient. The model is further validated by simulating the experimental data for the crystallization of a blend of poly(vinylidenefluoride)[PVDF] and poly(vinyl acetate)[PVAc] at various blending fractions.

Introduction

Polymer blending is a useful and economical way to produce new materials with a variety of properties. Many high-performance thermoplastics are prepared by the crystallization of polymer blends. The polymer−polymer interactions during crystallization can alter crystal structure, thermal stability, and mechanical properties such as rigidity and toughness. Understanding how adding a polymer component affects the morphology, crystallization, and mechanical and thermal properties of the polymer blend is a significant scientific challenge. To explore the crystallization kinetics of neat polymer melt, a cluster size distribution approach for nucleation accompanied by crystal growth and Ostwald ripening has been developed.[1] Polymer nucleation and crystal growth involve the dynamics of polymer chains, including the folded chain structures. Population balances equations based on crystal size distribution, and the concentration of amorphous polymer segments were established. The related moment and governing differential equations were also solved numerically under isothermal and nonisothermal conditions.[2,3] The approach presented a fundamental, quantitative explanation for the mechanism of nucleation and crystal growth. In the current work, we extend this approach to the application of polymer blend crystallization. The miscibility of polymer blends complicates the kinetics and dynamics of crystallization. Understanding how the addition of one component affects the crystallization behavior of the other can potentially be used to design and develop new types of high-performance polymer materials and to control product properties, e.g., microscopic structure, average size of polymer crystals, and crystal-size polydispersity.

Several studies have investigated the crystallization of neat polymer,[4−7] but binary polymer blend crystallization has received less attention. Experimental investigations on the miscibility and crystallization of polymer blends have been reported occasionally,[8−11] but only a few studies have been directed toward fundamental theoretical investigations. The understanding of how the presence of one component affects the morphology and crystallization of the other is still not clear for polymer blends. Polymer crystallization involves two phenomena: nucleation and crystal growth. The addition of a second polymer alters the crystallization kinetics of polymer solute mainly through these two steps. The temperature dependence of crystallization rates for neat (unmixed) polymers is approximately parabolic; crystallization rate is zero at T_g (glass temperature) and T_m (melting temperature), and the maximum rate appears between these two points. The addition of a second polymer to a semicrystalline polymer can act as a diluent, causing either a decrease in crystallinity by decreasing crystal number concentration or an increase in crystallinity by increasing chain mobility. The existence of polymer−polymer interactions also influences the deposition mechanism, causing either an increase or decrease of the crystal growth rate.

For example, the spherulite radial growth rate of poly(ethylene methacrylate) was found to decrease as poly(ethylene oxide) is added as the binary component.[12] By contrast, the presence of poly(vinyl methyl ether) was found to enhance the spherulite growth rate of polystyrene.[13] Increases in the spherulitic growth rate and crystallinity were also found for poly(vinyl methyl ether) added as a second ingredient in isotactic polystyrene.[14]

* Corresponding author. E-mail: giridhar@chemeng.iisc.ernet.in. Telephone: 91-080-2293-2321. Fax: 91-080-2360-0683.

10.1021/jp062451x CCC: $33.50
Published on Web 07/14/2006

The miscibility and crystallization of PES poly(ethylene succinate) (PES)and poly(vinyl phenol) (PVPh) blends[15] was investigated, and it was found that the growth rate of neat PES was higher than that of blended PES crystallized at the same temperature, which indicates that the addition of PVPh reduces the spherulite growth of PES in blends. The Avrami exponent was almost the same despite the blend composition and crystallization temperature.

A theoretical model was developed by Rostami[16] to explain the slower rate of spherulite growth in thermodynamically miscible blends of semicrystalline and amorphous polymers. Harris and Robeson[17] proposed a hypothesis to explain the enhancement of the crystallinity of a crystallizable component diluted with a miscible polymer. The interlamellar region, which contains the amorphous fraction, increased as the amorphous component is added to semicrystalline polymer. The increased amorphous fraction reduces the glass-transition temperature and lends additional mobility to the crystallizable ingredient, thus allowing a higher fraction of this ingredient in the crystalline phase.

For immiscible polymer blends, crystallization occurs within a single phase domain of a single component. The miscibility and crystallization of PHBV poly(3-hydroxybutyrate-*co*-hydroxyvalerate) (PHBV) and poly(ϵ-caprolactone) (PCL) blends were investigated, and these two polymers were not miscible.[18] The crystallization of the blends was studied using a two-step process: as the blend was cooled, the component with higher melting temperature crystallized first and the lower melting component crystallized later. The crystallization rate of PHBV decreased with increase of PCL, while the crystallization rate of PCL increased with increasing PHBV fraction. The Avrami exponent for crystallization of PCL varied as the component fraction of PHBV changed and was almost the same for crystallization of PHBV as fraction of PCL changed.

In this study, we focus on the crystallization kinetics of binary miscible polymer blends; immiscible blends present additional difficulties that will be addressed in future work. Our approach is to represent the dynamics and kinetics of nucleation and growth by a cluster size distribution model for binary polymer blends. The influence of the blending fraction on crystallization is incorporated into the effect of blending on the nucleation and crystal growth rates.

Theoretical Model

The addition of a second polymer can act as a diluent, either decreasing crystallinity by decreasing concentration of crystallizable component and nuclei numbers or increasing crystallinity by enhancing nucleation rate or increasing chain mobility. Five patterns of crystallinity development are identified upon addition of a crystallizable polymer additive:[19] (1) the diluent does not affect the crystallization, (2) the diluent retards the crystallization rate, (3) the diluent prevents crystallization (particularly at high concentrations), (4) the diluent accelerates crystallization, and (5) the diluent provides enough thermal mobility to cause crystallization of a normally noncrystalline polymer. As mentioned, the addition of a second polymer ingredient affects crystallization mainly through nucleation and crystal growth rates. We use classical nucleation theory to account for the nucleation of polymer blends. The nucleation rate, according to classical nucleation theory,[20] can be represented as the flux over the energy barrier W^*,

$$I = k_n \exp(-W^*/RT) \tag{1}$$

with prefactor

$$k_n = (m^{(0)})^2 (2\sigma x_m/\pi)^{1/2} \rho^{-1} \tag{2}$$

and

$$W^* = 4x_m \delta \sigma^2/[\rho RT \ln(m^{(0)}/m_{eq}^{(0)})] \tag{3}$$

Here, $m^{(0)}$ is the bulk concentration of amorphous polymer segments in the miscible polymer blend, σ accounts for the interfacial energy of nucleus, δ represents the thickness of the crystalline lamellae, and x_m is the molecular weight of polymer segments. The thickness δ of the crystalline lamellae is approximated by the length of polymer segments, which is constant for a certain polymer. The equilibrium concentration $m_{eq}^{(0)}$, which is constant for a certain polymer blend, exclusively depends on crystallization temperature and the miscibility of the polymer blend. Thus, blending influences the nucleation rate through the dilution effect on the crystallized component concentration, $m^{(0)}$. As we increase the blending fraction of the second component, the nucleation prefactor k_n decreases, and so does the exponential term because of the increase of the nucleation energy barrier. Nucleation vanishes when the polymer concentration, $m^{(0)}$, is equal to or less than the equilibrium concentration, $m_{eq}^{(0)}$, because of the high energy barrier.

The addition of a second component affects crystal growth by altering the growth rate coefficient and deposition rate driving force. As proposed in our previous studies,[1−3] crystal growth is represented by a reversible mechanism of addition to and separation from nuclei. The polymer−polymer interaction introduced by blending may affect the deposition and, consequently, alter the growth rate coefficient k_g. Thus, the established population balance equation in our previous work[1−3] can be applied to polymer blends. Reasoned thusly, the governing equations for crystallization of neat polymer and polymer blends are the same, and the mixing effects are incorporated into the evaluation of $m^{(0)}$, $m_{eq}^{(0)}$, and growth rate coefficient $k_g(x)$. The governing equations are

$$\partial c(x, t)/\partial t = -k_d(x)\, c(x, t) + \int_x^\infty k_d(x')\, c(x', t)\, \delta(x - (x' - x_m))\, dx' - k_g(x)\, c(x, t)\, m^{(0)} \int_0^\infty \delta(x' - x_m)\, dx' + m^{(0)} \int_0^x k_g(x')\, c(x', t)\, \delta(x - x_m)\, dx' + I\, \delta(x - x^*) \tag{4}$$

and

$$\partial m(x, t)/\partial t = -m^{(0)}(t) \int_0^\infty k_g(x')\, c(x', t)\, dx' + \int_x^\infty k_d(x')\, c(x', t)\, \delta(x - x_m)\, dx' - I\, \delta(x - x^*)\, x^*/x_m \tag{5}$$

where I accounts for nucleation rate given in eq 1. A general expression for growth rate coefficient $k_g(x)$ is a power law dependence on crystal mass x, $k_g(x) = \kappa_g x^\lambda$, where the value of power exponent λ depends on the deposition mechanism. A polymer segment that deposits on a crystal surface diffuses through the solution to react on the crystal surface; such diffusion-controlled reactions have a rate coefficient represented by

$$k_g = 4\pi D r_c \tag{6}$$

where D is the diffusion coefficient. The crystal size is related to its mass x by $r_c = (3x/4\pi\rho_c)^{1/3}$, in terms of crystal density ρ_c, which is constant at a given temperature. Thus, the power λ

$= {}^1/_3$ represents diffusion-controlled crystal growth. In dilute solutions, D is linearly dependent on the blending fraction.[21,22] However, the polymer segment−segment interactions complicate the determination of the diffusion coefficient in polymer−polymer mixtures. We may express the diffusion coefficient in terms of tracer diffusion of each component D^*, degree of polymerization N, blending fraction ϕ, and the Flory−Huggins interaction parameter χ,[23−26]

$$D = (D_A{}^* N_A \phi_B + D_B{}^* N_B \phi_A)(\phi_A/N_B + \phi_B/N_A - 2\phi_A\phi_B\chi) \quad (7)$$

with subscripts A and B representing the two polymer components. As the activation energy for the growth coefficient accounts for activated diffusion, eq 7 can be expanded into a polynomial in the blending fraction $\phi_A = 1 - \phi_B$,

$$D = D_0 \exp(-E/RT)\,(1 + a_1\phi_A + a_2{\phi_A}^2 + a_3{\phi_A}^3) \quad (8)$$

where a_1, a_2, and a_3 are constants for a certain polymer blend depending on D^*, N, and χ. The diffusion activation energy E also varies as the blended polymer or its fraction changes, leading to the variation of growth rate coefficient. Substituting $r_c = (3x/4\pi\rho_c)^{1/3}$ and eq 7 into eq 6 gives a detailed expression for the growth rate coefficient

$$k_g(x) = \gamma x^{1/3} \exp(-E/RT)(1 + a_1\phi_A + a_2{\phi_A}^2 + a_3{\phi_A}^3) \quad (9)$$

with $\gamma = 4\pi D_0(3/4\pi\rho_c)^{1/3}$. The volume fraction ϕ_A can also be related to $m^{(0)}$, the molar concentration of component A, by

$$m^{(0)} = \phi_A/\nu_m \quad (10)$$

where ν_m is the molar volume of crystallized component A. Thus, the growth rate coefficient can be represented in terms of $m^{(0)}$ as

$$k_g(x) = \gamma x^{1/3} \exp(-E/RT)(1 + b_1 m^{(0)} + b_2 m^{(0)2} + b_3 m^{(0)3}) \quad (11)$$

with $b_1 = a_1/\nu_m$, $b_2 = a_2/\nu_m{}^2$, and $b_3 = a_3/\nu_m{}^3$. When the growth is limited by the crystal surface, the rate coefficient is proportional to the crystal surface area, $r_c{}^2$, so that the power exponent of growth is $\lambda = {}^2/_3$, which represents the surface-controlled deposition rate coefficient. If the deposition rate is independent of the crystal surface area, then the power exponent of growth is $\lambda = 0$, indicating that crystal growth rate is independent of mass. With the definition of dimensionless quantities as follows

$$C = cx_m/\mu_\infty,\ C^{(n)} = c^{(n)}/\mu_\infty\, x_m{}^n,\ \xi = x/x_m,\ \theta = t\gamma\mu_\infty x_m{}^\lambda,$$
$$S = m^{(0)}/\mu_\infty,\ \Theta = T/T_m,\ w = 2\sigma_0\,(x_m b/\rho)^{1/2}/RT_m,$$
$$J = I/\gamma\mu_\infty{}^2 x_m{}^\lambda,\ \epsilon = E/RT_m,\ h = \Delta H/RT_m \quad (12)$$

Equations 4 and 5 are rewritten as,

$$dS(\theta)/d\theta = (1 + d_1S + d_2S^2 + d_3S^3)\exp(-\epsilon/\Theta)\,[-S(\theta) + \exp(-h/\Theta)]C(\lambda) + J\xi^* \quad (13)$$

and

$$\partial C(\xi,\theta)/\partial\theta = (1 + d_1S + d_2S^2 + d_3S^3)\,S(\theta)\exp(-\epsilon/\Theta)\,(-\xi^\lambda C(\xi,\theta) + (\xi-1)^\lambda C(\xi-1,\theta)) - \xi^\lambda \exp(-(\epsilon+h)/\Theta)C(\xi,\theta) + (\xi+1)^\lambda \exp(-(\epsilon+h)/\Theta)C(\xi+1,\theta) - J\delta(\xi-\xi^*) \quad (14)$$

with $d_1 = b_1\mu_\infty$, $d_2 = b_2\mu_\infty{}^2$, and $d_3 = b_3\mu_\infty{}^3$. The scaled nucleation rate J can be written in terms of supersaturation S, interfacial energy w, temperature Θ, and phase transition enthalpy h

$$J = J_0(1-\Theta)^{n/2}\,S^2 \exp[-(w(1-\Theta)^n/\Theta)^2/(\ln S + h/\Theta)] \quad (15)$$

with

$$J_0 = (2\sigma_0/\pi)^{1/2}/\rho\gamma x_m{}^{\lambda-1/2} \quad (16)$$

The parameter n is the exponent of temperature in the expression for interfacial energy.[1,2] For the simple case of surface independent deposition, $\lambda = 0$, the moment technique can be used to rewrite the population balance equations as

$$dS(\theta)/d\theta = (1 + d_1S + d_2S^2 + d_3S^3)\exp(-\epsilon/\Theta)\,[-S(\theta) + \exp(-h/\Theta)]C^{(0)} + J\,\xi^* \quad (17)$$

$$dC^{(0)}(\theta)/d\theta = J \quad (18)$$

$$dC^{(1)}(\theta)/d\theta = -(1 + d_1S + d_2S^2 + d_3S^3)\exp(-\epsilon/\Theta)[-S(\theta) + \exp(-h/\Theta)]C^{(0)} - J\,\xi^* \quad (19)$$

For any nonzero λ, the moment equations lack closure, thus a numerical technique is required to solve eqs 13 and 14.

The number of macromolecules in the critical crystal nucleus is

$$\xi^* = [w(1-\Theta)^n/\Theta\,(\ln S + h/\Theta)]^2 \quad (20)$$

which varies with time because of the time dependence of the scaled number of crystallizing polymers S and is strongly dependent on temperature. In terms of the initial number of polymer molecules S_0, the scaled mass conservation for a closed system follows from the population balance equations, eqs 17 and 19

$$C^{(1)}(\theta) + S(\theta) = C_0{}^{(1)} + S_0 \quad (21)$$

where $C_0{}^{(1)}$ is the initial cluster mass, representing heterogeneous nuclei and seeds, and is zero for homogeneous nucleation, and S_0 is the initial number of polymer molecules. The degree of crystallinity, X, is defined as the ratio of the mass crystallized at time t divided by the total mass crystallized,

$$X = (C^{(1)} - C_0{}^{(1)})/(C_{eq}{}^{(1)} - C_0{}^{(1)}) \quad (22)$$

Substitution of the mass conservation equation, eq 21, simplifies the above equation to

$$X = (S_0 - S(\theta))/(S_0 - e^{-h/\Theta}) \approx 1 - S/S_0 \quad (23)$$

The growth rate coefficient is not the only parameter subject to change under different blend fractions, although only its dependence on blend fraction is mathematically approximated in the population balance equations. Melting temperature, phase transition enthalpy, and activation energy may also change with

TABLE 1: Parameter Values Used in the Model for Figure 1

ϕ_A	S_0	ϵ	h	Θ	$C_0^{(0)}$	$C_0^{(1)}$	J_0	λ	w	n	d_1	d_2	d_3
1.00	10	2.0	10	0.950	0	0	10^6	0	2.0	20	1	0	0
0.90	9	2.5	9	0.955	0	0	10^6	0	2.0	20	1	0	0
0.80	8	3	8	0.96	0	0	10^6	0	2.0	20	1	0	0
0.70	7	3.5	7	0.965	0	0	10^6	0	2.0	20	1	0	0

blending fraction, e.g., the melting temperature of poly(vinylidenefluoride)[PVDF]/poly(vinyl acetate)[PVAc] blends varies from 170.7 °C to 152.4 °C as the fraction of PVAc increases from 0 to 30%.[27] To keep the governing equations simple, we consider the effects of the blending fraction on those parameters in computation rather than approximate them mathematically in the population balance equations.

Results and Discussion

For the crystallization of miscible polymer blends, we are concerned with the effect of blending on the kinetics of crystallization for the easily crystallizing component, i.e., the component crystallizing at the relatively higher temperature. The increase of the second ingredient fraction, according to eqs 1, 2, and 3, leads to decreasing nucleation rate because of the dilution of concentration $m^{(0)}$. The dilution also slows the crystal growth rate by decreasing the deposition rate and the driving force, $-S(\theta) + \exp(-h/\Theta)$. Thus, by incorporating the blending effects for melting temperature T_m, enthalpy of fusion ΔH, and activated diffusion energy ϵ, introducing a second polymer component generally delays the crystallization by decreasing nucleation and crystal growth rates.

For the simple case of surface-independent deposition ($\lambda = 0$), the governing moment eqs 17−19 are solved by NDSolve in Mathematica to assess the effect of blending on nucleation and crystal growth rate. The moment method provides an easy and quick model for polymer crystallization with surface-independent crystal growth ($\lambda = 0$). However, a general approach is to solve the equations numerically based on methods described previously.[1,3] The differential eq 19 is solved by the Runge−Kutta technique with an adaptive time step and $C(\xi, \theta)$ is evaluated at each time step sequentially. The mass variable (ξ) is divided into 5000 intervals, and the adaptive time (θ) step varied from 10^{-5} to 10^{-2}, ensuring stability and accuracy at all values of the parameters. At every time step, the mass conservation (eq 21) was verified. The numerical results are further validated by comparison with the analytical moment solutions obtained for $\lambda = 0$.

Our choice of parameters is based on earlier papers[1−3] and experimental measurements.[28] Previous work suggested a value[1] $n = 20$ in eqs 15 and 20 to represent the temperature dependence of interfacial energy. The interfacial energy parameter w, written in terms of density, is chosen to be $w = 2$. The molar enthalpy of phase transition h is usually about 10. The activation energy, ϵ, for growth rate is typically smaller than h, and a constant nucleation rate prefactor, $J_0 = 10^6$, is proposed. The values of various parameters used in the model are summarized in Table 1. There are no particles present initially for homogeneous nucleation, thus the initial conditions are $S(\theta = 0) = S_0$, $C^{(0)}(\theta = 0) = 0$, and $C^{(1)}(\theta = 0) = 0$.

Figure 1 presents the computational results of crystallization time evolution as the fraction of the second polymer component

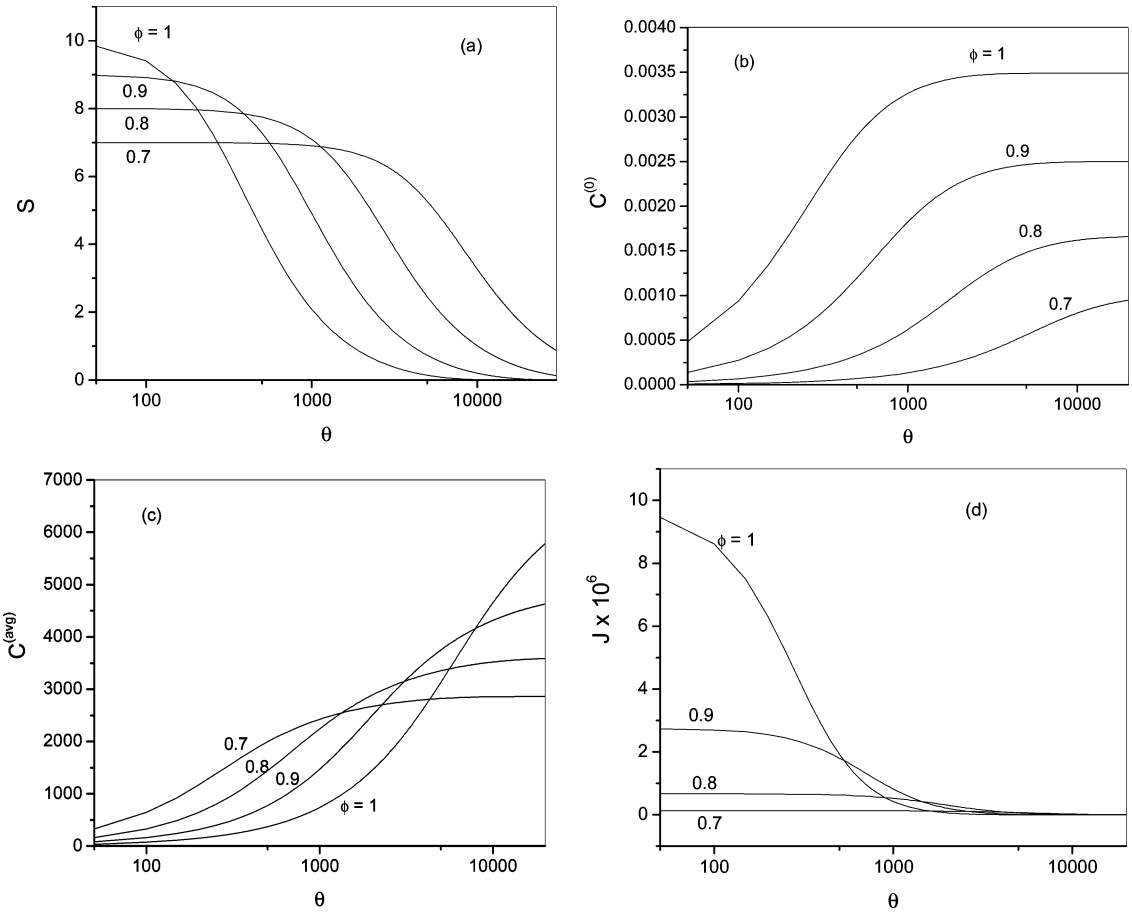

Figure 1. Time evolution of (a) supersaturation, (b) number of crystals, (c) average crystal size, and (d) nucleation rate for various blending fractions (parameters are listed in Table 1).

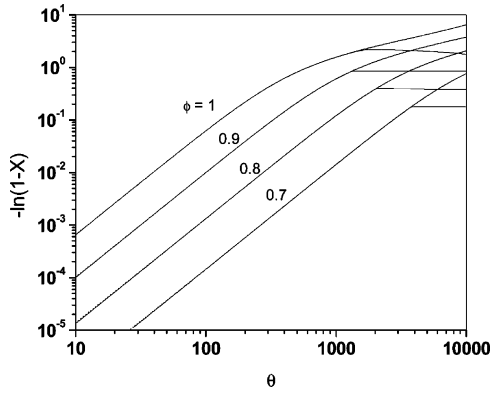

Figure 2. Avrami plot showing the time evolution of crystallinity comparing the moment solution (solid line) and the numerical solution (dotted line) with the parameters listed in Table 1.

changes. The initial values of scaled solute concentrations, $S_0 = 10$, 9, 8, and 7, correspond to the second component fraction of 0% (neat polymer), 10, 20, and 30%, respectively. The parameters d_1, d_2, and d_3, which depend on polymer physical properties, are chosen to equal 1.0, 0, and 0, respectively. Such a linear approximation for the diffusion coefficient D may constrain applicability to a certain range of blend fraction. For a miscible blending system, crystallization is initiated only above the critical blending fraction where the two components are in equilibrium. Most of crystallization processes are initiated by cooling; and polymer−polymer solutions become supersaturated as the temperature decreases. Consequently, the supersaturated component begins to nucleate only after the fraction of crystallized component in the liquid phase decreases to the equilibrium blending fraction corresponding to the crystallization temperature. Thus crystallization of miscible polymer blends occurs only within a certain range of blending fraction.

Figure 1a shows the time evolution of supersaturation S. The consumption rate of free solute (in the amorphous state) decreases as the fraction of the second polymer increases because the neat polymer has the largest solute consuming rate. Compared with neat polymer melt, the blended system requires more time to complete the crystallization. The time evolution of crystal number and crystal size is represented in Figure 1b and c. The influence of the second polymer in the blend (Figure 1b) shows that the fraction increase of the second polymer dilutes the solute concentration. Meanwhile, the initial critical size ξ_0^* (eq 20) is also subject to increase because the supersaturation decreases as the blending fraction increases. Figure 1c presents the time evolution of the average crystal size, indicating the influence of blending fraction on crystal growth rate. The rise of the second polymer component fraction slows the crystal growth rate by decreasing the growth rate coefficient and deposition rate driving force. As a consequence, the smallest average crystal size at a blending fraction of the second component under 30% is observed. The influence of the second polymer in the blend shows that the fraction increase of the second polymer decreases nucleation rate, as shown in Figure 1d.

The model is also used to represent the Avrami plots of the crystallinity time evolution, as shown in Figure 2. The evolution of crystallinity with time integrates the blending effects on both nucleation and crystal growth and indicates the negative influence on crystallization time for the second polymer component. The variation of the blending fraction does not affect the Avrami exponent significantly. Denucleation, the reverse of nucleation, occurs when the crystal size is smaller than the critical nucleus size. Denucleation has considerable influence on the characteristic Avrami plots, especially at the end of crystallization when denucleation dominates over nucleation. At the beginning of crystallization, most polymer crystals are larger than the critical crystal size, thus denucleation, compared with nucleation, is negligible. The critical crystal size, however, increases as the supersaturation declines when polymer deposits on the crystal, thus more crystals become smaller than the critical size. These unstable crystals will dissolve rapidly. At the end of crystallization, denucleation and ripening become dominant because the supersaturation is close to unity, and consequently, nucleation vanishes. Figure 2 presents the effect of denucleation by comparison of moment and numerical solutions. The solid lines represent the characteristic Avrami plots of moment solutions for which denucleation is not considered. The dotted lines represent the numerical solutions that account for denucleation. At the beginning, the denucleation rate is small and the moment solution matches the numerical solution very well because the small denucleation rate delays the dominating influence of nucleation.[29] As supersaturation decreases, the discrepancy between moment solution and numerical solution caused by denucleation becomes apparent at long times. The numerically computed crystallinity reaches its asymptote, whereas the crystallinity computed by the moment method continues to increase.

Figure 1 presents model predictions when the diffusion coefficient D is approximated by a linear dependence on blending fractions, ϕ_A, and Figure 3 shows the time evolution of crystallinity and crystal size based on the linear approximation of diffusion coefficient by varying d_1 in the range of 0.1−10

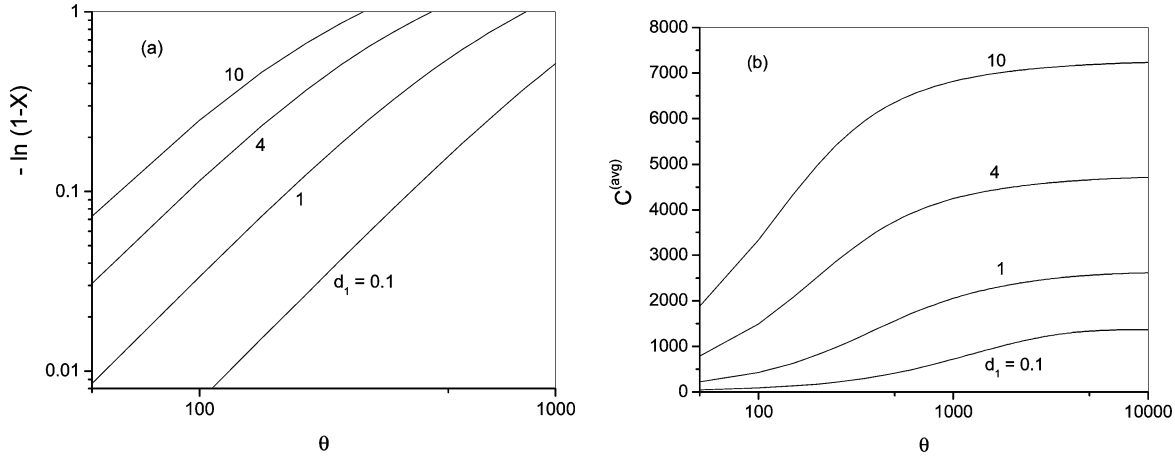

Figure 3. Effect of d_1 on the time evolution of (a) crystallinity and (b) crystal size with $\phi_A = 0.80$ and the parameters listed in Table 1.

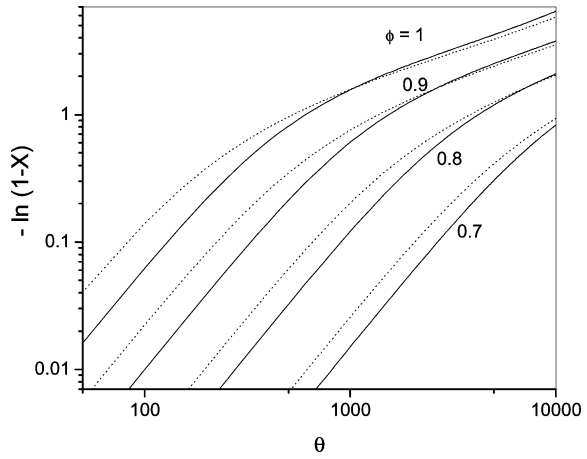

Figure 4. Comparison between linear and nonlinear expression for diffusion coefficient with $C_0^{(0)} = 0$, $C_0^{(1)} = 0$, $\phi_A = 0.80$, $J_0 = 10^6$, $\lambda = 0$, and $n = 20$. The dotted line is the linear approximation for D ($d_1 = 1$, $d_2 = 0$, and $d_3 = 0$) and the solid line represents the polynomial expression for D with $d_1 = 1$, $d_2 = -0.02$, and $d_3 = 0.02$.

(see eqs 13 and 14). It is observed that a stronger dependence of the diffusion coefficient on the blending fraction leads to faster crystallization rates. The slope of the Avrami plot (Avrami exponent) does not depend on d_1, as shown in Figure 3a. The effect of d_1 on average crystal size is presented in Figure 3b. According to the linear expression of the diffusion coefficient, a large value of d_1 leads to an increase in the diffusion coefficient, resulting in a larger average crystal size, as shown in Figure 3b.

We next determine the effect of a polynomial dependence of D on blending fractions. The time evolution of crystallization based on linear and polynomial expressions for diffusion coefficient D is shown in Figure 4. The polynomial expression for diffusion coefficient does not lead to a significant variation in Avrami exponent, suggesting that the linear expression is a valid approximation.

The presence of the second polymer in the blend[19] may either decrease or increase the absolute value of T_g and T_m of the semicrystalline ingredient, depending upon the difference between the isothermal crystallization temperature, T_i, and $(T_g + T_m)/2$. Depending on whether this difference increases or decreases with the addition of the second ingredient, the crystallization rate decreases or increases, respectively. In the proposed model, eq 19 indicates that the crystal growth and crystallization rate would increase or decrease depending on whether Θ increases or decreases with the blending fraction, respectively, consistent with the observed experimental data.[19]

TABLE 2: Melting Temperature T_m, Heat of Fusion ΔH_m, and Diffusion Activation Energy E of PVDF and PVDF/PVAc Blends under Different Blending Fractions[27] and the Parameter Values Used in the Model to Fit the Experimental Measurements in Figure 5[a]

PVDF/PVAc	T_m/°C	ΔH_m/J/g	E/J/g	ϕ_A	S_0	ϵ	h	Θ
100/0	170.7	64.54	0.96	1.00	10	1.3	10	0.949
90/10	168.4	55.27	1.03	0.90	9	1.4	8.56	0.954
80/20	167.3	42.69	2.05	0.80	8	2.8	6.61	0.956
70/30	152.4	40.06	5.30	0.70	7	7.5	6.21	0.989

[a] The other parameters are the same as listed in Table 1.

The validity of the distribution kinetics model is also examined by comparison with the experimental data[27] of the PVDF/PVAc blend (Figure 5), where Θ decreases with increasing blending fraction, and therefore, the crystallization rate decreases with the blending fraction. The simulation results are based on dimensionless time $\theta = t\gamma\mu_\infty x_m^\lambda$, so a transposition of the original experimental data, based on real time, is applied to compare with simulations. According to the definition of dimensionless time, a horizontal transposition of $\log(\gamma\mu_\infty x_m^\lambda)$ units is applied to the experimental measurements to convert the experimental data into plots based on dimensionless time θ. The points are experimental data,[27] and the model parameters are listed in Table 2. A moment solution with surface-independent crystal growth ($\lambda = 0$) does not fit the experimental data (Figure 5a), so $\lambda = 1/3$ is chosen[3] and the population balance equations are solved numerically. The measured horizontal transposition is unity, independent of the blend fraction or temperature. Good agreement between experimental data and simulation results (Figure 5b) with $\lambda = 1/3$ is observed, indicating that the crystal growth for the PVDF/PVAc blending system is diffusion dominated.

Conclusions

On the basis of a previous distribution kinetics approach, we have investigated the crystallization kinetics of miscible polymer blends. This model accounts for the effects of polymer blending on nucleation and crystal growth rates. Adding a second polymer influences the crystallization mainly through thermodynamics and kinetics (equilibrium solubility and deposition mechanism). These effects are incorporated by varying the initial values of monomer concentration and growth rate coefficient. Assuming that the deposition mechanism does not change during crystallization, we have investigated the crystallization kinetics for various blending fractions. Computation results indicate that increasing the second polymer fraction leads to the decrease of both nucleation and crystal growth rates, while the Avrami

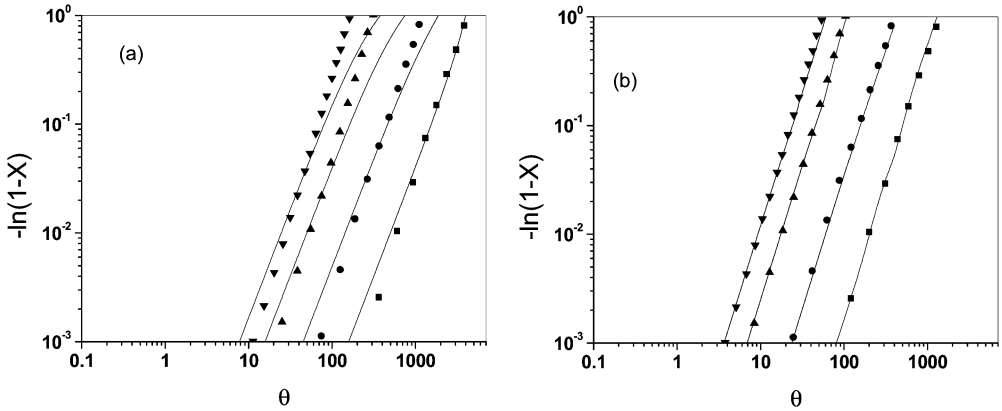

Figure 5. Model prediction of the experimental data of the PVDF/PVAc blend with different blending fractions with (a) $\lambda = 0$ and (b) $\lambda = 1/3$; (▼): PVDF/PVAc = 100/0, (▲): PVDF/PVAc = 90/10 (●): PVDF/PVAc = 80/20, (■): PVDF/PVAc = 70/30.

exponent does not change. The diffusion coefficient plays an important role in determining the time evolution of polymer blends because of the strong polymer−polymer interactions. A polynomial expression and a linear approximation for the diffusion coefficient on the blending fraction are compared, and it is found that the linear expression is an adequate approximation. The model is used to simulate the experimental data of the time evolution of crystallinity for the blend of poly(vinylidenefluoride) [PVDF] and poly(vinyl acetate) [PVAc] at various blending fractions.

References and Notes

(1) Yang, J.; McCoy, B. J.; Madras, G. *J. Chem. Phys*. **2005**, *122*, 64901.
(2) Yang, J.; McCoy, B. J.; Madras, G. *J. Chem. Phys.* **2005**, *122*, 244905.
(3) Yang, J.; McCoy, B. J.; Madras, G. *J. Phys. Chem. B* **2005**, *109*, 18550.
(4) Toma, L.; Toma, S.; Subirana, J. A. *Macromolecules* **1998**, *31*, 2328.
(5) Leisen, J.; Beckham, H. W. *Macromolecules* **2004**, *37*, 8028.
(6) Kratochvil, J.; Sikora, A.; Baldrian, J.; Dybal, J.; Puffr, R. *Polymer* **2000**, *41*, 7653.
(7) Ciora, R. J.; Magill, J. H. *Macromolecules* **1990**, *23*, 2350.
(8) Wang, H.; Shimizu, K.; Kim, H.; Hobbie, E. K.; Wang, Z.; Han, C. C. *J. Chem. Phys.* **2002**, *116*, 7311.
(9) Su, C.; Shih, C. K. *Colloid. Polym. Sci.* **2005**, *283*, 1278.
(10) Hsu, J.; Nandan, B.; Chen, M.; Chiu, F.; Chen, H. *Polymer* **2005**, *46*, 11837.
(11) Yi, J. Z.; Goh, S. H. *Polymer* **2003**, *44*, 1973.
(12) Cimmino, S. *J. Polym. Sci., Polym. Phys.* **1999**, *27*, 1781.
(13) Bartczak, Z.; Gaeski, A.; Martuscelli, E. *Polym. Eng. Sci*. **1984**, *24*, 563.
(14) Martuscelli, E.; Sellitti, C.; Silvestre, C. *Macromol. Chem., Rapid Commun*. **1985**, *6*, 125.
(15) Qiu, Z.; Fujinami, S.; Komura, M.; Nakajima, K.; Ikehara, T.; Nishi, T. *Polymer* **2004**, *45*, 4515.
(16) Rostami, S. *Polymer* **1990**, *31*, 899.
(17) Harris, J. E.; Robeson, L. M. *J. Polym. Sci., Polym. Phys.* **1987**, *25*, 311.
(18) Qiu, Z.; Yang, W.; Ikehara, T.; Nishi, T. *Polymer* **2005**, *46*, 11814.
(19) Long, Y.; Shanks, R. A.; Stachurski, Z. H. *Prog. Polym. Sci*. **1995**, *20*, 651.
(20) Oxtoby, D. W. *J. Phys.*: *Condens. Matter* **1992**, *4*, 7627.
(21) Yamakawa, H. *Modern Theory of Polymer Solution*; Harper & Row: New York, 1971; p 262.
(22) Cussler, E. L. *Diffusion, Mass Transfer in Fluid System*; Cambridge University Press: New York, 1997; p 118.
(23) White, D. M. *Phys. Rev. Lett.* **1986**, *57*, 1312.
(24) Kanetakis, J.; Fytas, G. *J. Chem. Phys.* **1987**, *87*, 5048.
(25) Brochard, F. *Macromolecules* **1983**, *16*, 1638.
(26) Flory, J. *Principles of Polymer Chemistry*; Cornell University Press: Ithaca, NY, 1953; p 507.
(27) Chiu, H. *J. Polym. Res.* **2002**, *9*, 169.
(28) Xiao, J.; Zhang, H.; Wan, X.; Zhang, D.; Zhou, Q.; Woo, E. M.; Turner, S. R. *Polymer* **2002**, *43*, 7377.
(29) Madras, G.; McCoy, B. J. *J. Chem. Phys*. **2002**, *117*, 8042.